Comparison of Rayleigh-scatter lidar temperature climatologies in the mesosphere and lower thermosphere between the traditional reduction method and the new optimal estimation method.

Abstract

An optimal estimation method (OEM) was used to obtain all-night temperature profiles from Rayleigh-scatter lidar (RSL) observations obtained by the original and updated lidar systems at Utah State University (USU). These data were used to produce annual climatologies of temperatures above USU. The climatology of temperatures from the original lidar, which operated from late 1993 through 2004, was compared with the climatology produced using the widely used Hauchecorne-Chanin method (HC). This comparison highlights the similarities at lower altitudes and differences, which start between 70 km and 80 km and extend to the top altitudes with the OEM temperatures warmer on average than those of the HC. The differences between methods are likely due to the reliance of the HC on a seeding temperature at the top altitude which likely has a large influence on the temperatures at the top 10 km. OEM and HC temperature climatologies were also produced using observations from the upgraded RSL at USU, which operated from early 2014 to early 2015. Like the original climatology, the newer climatology was seen to differ most at higher altitudes. The OEM climatologies from the original and newer data sets were compared, showing good agreement in the location of the summer mesopause but with colder temperatures in this region from the newer observations.

1. Introduction

Rayleigh-scatter lidar (RSL) is an important tool for studying the middle atmosphere. It is uniquely capable of observing the upper portion of the stratosphere, the entirety of the mesosphere and the lower thermosphere with high temporal and height resolution. RSL has been used mainly in studying temperature characteristics in the middle atmosphere. Study topics have included atmospheric gravity waves (Hauchecorne et al., 1987; Kafle 2009; Sica & Argall, 2001), model validation (Ehard et al., 2018; Wing et al., 2018 a&b), and long-term temperature trends (Hauchecorne et al., 1991). A useful tool for studying annual temperature trends is by creating a temperature climatology (Herron, 2007; Herron & Wickwar, 2018; Argall & Sica, 2011; Jalali et al., 2018). An annual temperature climatology consists of averaging temperature profiles from each day, week or month over the entire data set. One such climatology was done by Herron (2007) (Herron and Wickwar, 2018) which used observation from over 900 nights of RSL data between late 1993 through 2004.

Hauchecorne and Chanin (1980) (HC) introduced a robust temperature retrieval method for the RSL observations. This widely used method uses a top down method integrating from the top altitude down, requiring an initial temperature at the top altitude. The lidar equation is utilized along with the assumptions that the atmosphere consists of an ideal gas in hydrostatic equilibrium. Recently, a new method has been introduced which uses an optimal estimation method (OEM) to retrieve atmospheric temperatures. The method was developed by Rogers (2000) for use in the radiometric community and applied to RSL temperature reduction by Sica and Haefle (2015). Some key improvements over the HC method include a robust

uncertainty budget which provides uncertainties in instrument performance, atmospheric transmission, Rayleigh-scatter cross section along with statistical uncertainties and a well-defined limit for the topmost altitude in the temperature profile. Originally developed for use with the MATLAB scientific programming language, I have ported the OEM into Python and used it to reduce the USU RSL observations. The conversion to Python is based on the goal of providing an open-source version of the OEM which removes the reliance on expensive software subscriptions.

For comparisons with the HC results from Herron (2007), a new climatology was produced in the same manner using OEM temperatures reduced from the original USU RSL observations. Jalali et al (2018) did a similar comparison between these methods using data from the Purple Crow lidar (PCL) at the University of Western Ontario, Canada (UWO), demonstrating good consistency with the HC method. Good agreement between the HC and OEM temperature climatologies using USU RSL observations, particularly for the first 40 km, was demonstrated in this study. A slight increase in the altitudes of the topmost valid temperatures was also demonstrated. In addition to the slight increase in altitude, the temperatures at the top altitudes are much less dependent on an a priori temperature value than in the HC method. An additional temperature climatology using both OEM and HC methods consisting of observations made using the upgraded lidar system (Sox, 2016), which extends about 20 km higher, up to 115 km, is also presented.

2. RSL Instrument

The original RSL on the Utah State University campus (41.74° N, 111.81° W) operated from August 1993 through November 2004. During this period there were two Nd:YAG lasers used at different times. The initial setup used a 24-watt Spectra Physics laser operating at 532 nm at a 30 Hz repetition rate. It was later replaced with an 18-watt Spectra Physics laser operating at 532 nm at a 30 Hz repetition rate. The telescope receiver consisted of a single 44 cm diameter mirror which focused light through a field stop, limiting the field of view to 3 times that of the 1-mrad divergence of the laser beam. The light was focused onto the plane of a mechanical chopper to prevent oversaturating the PMT detector with very intense light from scattering at lower altitudes. The light was then collimated and passed through a narrow bandpass filter, which isolated light at the laser wavelength, and then passed to a Peltier cooled photomultiplier tube (PMT). The signal was converted from analog to digital using a converter then sent to a multichannel scaler and stored into altitude bins of 37.5 m (125 ns sampling) and integrated over two minutes. The effective range of observation was from 45 km to above 90 km when the signal was integrated over an entire night. More details on the system are given by Wickwar et al., (2001) and Herron, (2004).

By 2014, the lidar system had been significantly upgraded. The new system combined both the 18-watt and 24-watt lasers for a total power of 42 watts. The receiver system was upgraded to four coaligned 1.25 m diameter mirrors, providing an effective aperture area of 4.9 m^2. A 1.5 mm diameter fiber optic was placed at the focal point of each mirror. The light from the four mirrors was then combined, focused on the chopper plane, collimated and directed onto the PMT. The increased power and aperture area extended the all night USU RSL observation range upward to ∼115 km. The bottom of the valid altitude range was moved up to 70 km in order to prevent signal from lower altitudes saturating the detector, preventing us from detecting the faint signal at the topmost altitudes. Over 100 nights of observations were made between 2014 and 2015. Sox (2016) provides extensive details on the upgraded lidar system. Another upgrade repurposed the 44 cm diameter mirror and added another detector system, lowering the bottom altitude to 40 km while overlapping

significantly with the signal from the 4-mirror telescope. This combined system showed that the range could be extended from 40 to 115 km. A future planned upgrade involving new detectors and interference filters should extend the top range upward to 125 km and lower the minimum range to 30 km.

3. Climatology

Creating a climatology of the temperature data is a technique used to model the expected behavior for the temperatures on a given day of the year. This provides a broad look at the quality of the data and a quick look at how the OEM compares with the HC method for temperature retrieval. It also provides a way to detect and compare individual profiles that differ significantly or demonstrate interesting behavior from the composite model profile for that night. The original eleven-year data set, consisting of over 1000 nighttime observations, provides an excellent foundation for a climatology.

The composite year climatology of USU RSL temperatures using the OEM retrieval method is created in the same way as the HC based climatology of Herron and Wickwar (2018). The temperatures were first averaged by day of year over the eleven years. A running average was then performed for each composite day using a 31-day window with each day at the center to produce a composite day representing each day of the year. Before any averaging is performed, outliers within the data set are filtered from use if the profile differs by more than 3 standard deviations from a monthly mean profile. This is done to exclude extreme temperature profiles to create a more likely representation of a typical year. Out of the 1090 available profiles, ~200 profiles were excluded using this process. Many of these excluded profiles contain erroneous temperatures mainly due to instrument errors or poor weather conditions. Some are likely due to anomalous temperatures caused by unknown, but real, sources, such as on the night of February 20, 2004 (Bentley et al. 2018). While many of these profiles were deemed as 'bad' nights (Herron, 2007), not all should be labeled as such and merit further investigation as they could represent real anomalous atmospheric behavior. As the purpose of a climatology is to present more normal behavior, these nights have been left out.

4. Results

4.1 Original Lidar Results

Figure 3.1 shows the temperature climatology for a composite year using the OEM. The climatology consists of ~890 nights of temperature observations from USU extending from 45 km to about 100 km in some cases. The summer mesopause (starting with the dark purple region), which contains the

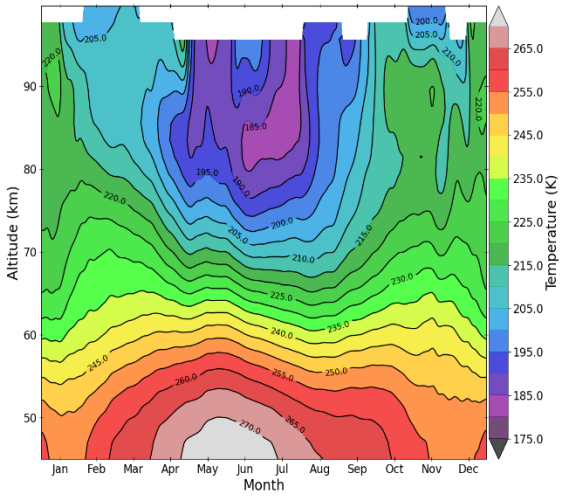

Figure 3.1: Temperature climatology of USU RSL temperatures reduced using OEM.

lowest temperatures in the mesopause, occurs from mid-April through mid-August, with the minimum temperatures (light purple region) occurring between mid-June through the end of July centered about roughly 83 km. Hints of lower temperatures in the spring and fall can be seen at the top altitudes. However, without being able to see higher we cannot say for sure

where the winter mesopause is located. We can only say that we expect it to be above 100 km.

Large temperature gradients occur in the summer between 50 km and 80 km. This is due to the high altitude of the summer stratopause, which is the hottest region of the stratosphere located around 45 km, and low altitude of the summer mesopause being closer together in altitude during the summer causing a higher rate of change in the temperature in this range. The top of the summer stratopause can be seen around 45 km from April through mid-August (light pink). From winter to spring we see higher relative temperatures descend from ~90 km down to ~65 km from late-January until early March respectively. Later, from fall to winter we see

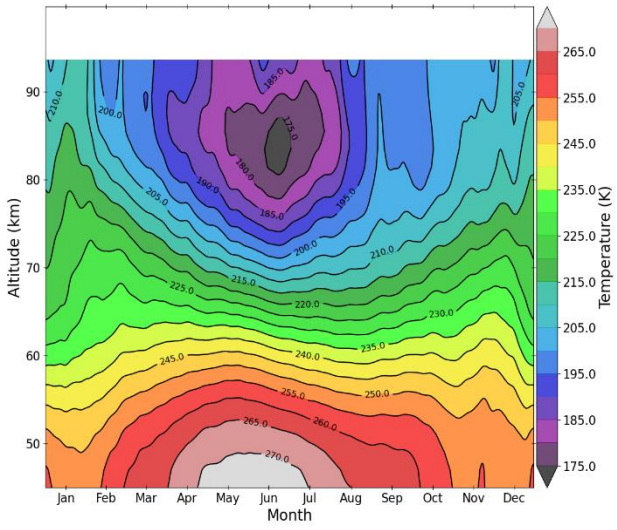

Figure 3.2: Temperature climatology of USU RSL temperatures reduced by Herron and Wickwar (2018) using the HC method.

higher relative temperatures ascending from ~55 km to ~87 km from mid-November until late-December respectively, with a low temperature trough creating a double peak appearance. Between these relative maxima we see a relative minimum occur in mid-January, most evident between 50 km and 70 km. Similar features were described by Herron and Wickwar (2018) which used the same data set but with the HC method to derive the temperatures. They also discuss the hotspot seen up to 50 km from late-December to early-January as a common feature among lidar groups and attribute the phenomena to Sudden Stratospheric Warmings (SSWs), pointing to a study of SSWs by Sox (2016) which also uses the USU RSL HC temperatures in the study.

Figure 3.2 shows the earlier climatology produced using temperatures reduced with the HC method for ~880 nights. The two temperature climatologies largely agree, with the summer mesopause (starting with the dark purple region) occurring around 83 km from mid-April through mid-August and the minimum temperatures centered around mid- to late -June. The summer stratopause around 45 km shows the warmest temperatures between mid-April and mid-July in both images. Above 80 km, however, the temperatures are, on average, higher in the OEM climatology. Only minor differences are apparent at lower altitudes, which show similar features discussed by Herron and Wickwar (2018). The

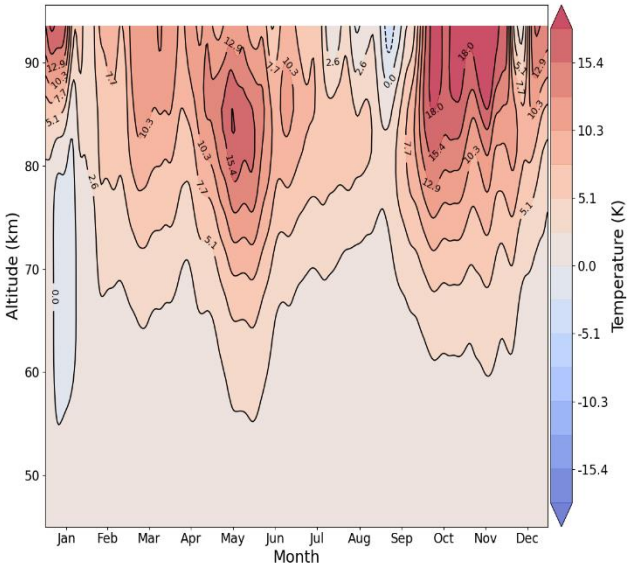

Figure 3.3: Plot showing the difference in temperature between OEM and HC. The overall positive temperatures differences mean that the OEM temperature reduction produced higher temperatures overall than the HC temperature reduction, particularly above 70 km.

differences between the OEM and HC derived climatologies are plotted in Figure 3.3.

Figure 3.3 was made by subtracting the HC composite temperatures from the OEM

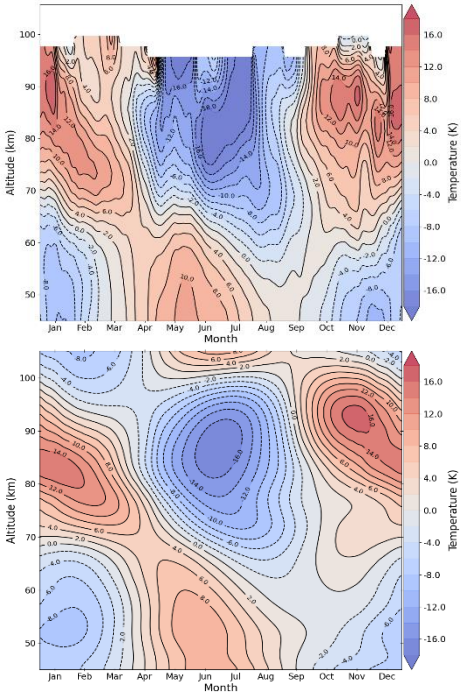

Figure 3.4: Contour plots showing the change in temperature in the climatology with respect to the annual mean temperature. Top: OEM temperature climatology. Bottom: MSIS2 temperature climatology.

composite temperatures. In this manner, the positive values denote higher OEM temperatures while the negative values denote higher HC temperatures. From the comparison we see that, overall, the OEM temperature climatology shows higher temperatures than the HC climatology. Below 70 km, however, the temperature differences are small (under ~2 K). The largest differences occur above 85 km from mid-September through November. Because the top altitude of the HC temperature retrieval is obtained externally (from a model or other source), many RSL researchers remove the top 10 km altogether from the retrieval in order to remove the possible effect of the seed temperature (Argall and Sica, 2007; Jalali et al., 2018; Sica and Haefele, 2015). This does not necessarily mean we should ignore the top 10 km in the HC temperature climatology, but that it could be a source of error attributing to the differences between the HC method and OEM method temperatures at these altitudes. The OEM temperatures do not rely wholly on the a priori temperature and so the values, with their uncertainties, can be used with confidence throughout the valid profile (Jalali et al., 2018; Sica and Haefele, 2015).

To further examine the temperature variations, a climatology of the change in temperature with respect to the annual mean of the composite year was created using the OEM composite temperatures. For comparison, a similar climatology was created using temperatures from MSIS2. This model was chosen for the comparison because it uses vast amounts of observations from various ground-based and space-based detectors (Emmert el al., 2020) to generate the model temperatures above USU. It is also the model used to provide the apriori temperatures used in the OEM temperature reduction. Figure 3.4 shows how the OEM temperatures change with respect to the OEM annual mean temperature (top) and how the MSIS2 model temperatures change with respect to the model annual mean temperature (bottom). Positive values indicate a nighttime temperature which is hotter than the annual mean temperature.

The summer mesopause can be identified in both the OEM and MSIS2 climatologies centered around July. The altitude of the mesopause centers around 85 km in both climatologies. The winter mesopause cannot be determined from the OEM data because it does not go high enough, but we can start to see it in the MSIS2 data centered around February. We see similar features in both plots showing higher temperatures descending from mid-January until early- to mid-June. MSIS2 shows this descent starting in October, with the local maximum in early-November around 92 km, and descending all through the winter until April whereas OEM shows a lot more structure in between October and April with a local maxima occurring around 88 km in late-December and around 90 km in mid-January. Counting from January until mid-June, the rate of descent for the high temperatures within the OEM climatology is -9.8 km per month while the rate for the MSIS2 climatology is slower at -7.1 km per month. In both the OEM and MSIS2 plots we see a larger temperature gradient in

the spring than in the fall below 60 km. The hot region in the summer below 50 km is centered around early-June in OEM but occurs ~15 days later in MSIS2.

At lower altitudes in Figure 3.4, we see a clear annual oscillation occurring in both OEM and MSIS2 plots with higher temperatures in summer and lower temperatures in winter below 60 km, the opposite being true between 70 km and 100 km. The OEM temperature difference climatology, however, shows higher order harmonics appearing above 70 km which are not apparent in the MSIS2 temperature difference climatology. A likely cause for the lack of higher order harmonics is the large amount of data averaging within the model (Emmert et al., 2020).

4.2 Upgraded Lidar Results

Figure 3.5 shows the OEM and HC temperature climatologies using observations from the high altitude lidar system which consisists of over 130 nights between 2014 and 2015. Due to the small number of nights in the data set, which do not quite cover an entire calendar year, this climatology is based on monthly averages instead of composite monthly averages about each night. Thus, because March and April do not have any data they are left blank. As with the lower altitude lidar temperature climatologies, these two plots show very similar temperatures, especially between May and November. The main differences occur, as with the low altitude temperatures, at the higher altitudes. In this case, they occur above 100 km. These differences occur mainly during the winter months and show a much higher temperature in the HC method. Large differences at high altitudes were also seen, and discussed, in the comparisons from the original lidar data. It is important to note that both the OEM and HC methods take account of the change in neutral atmosphere composition

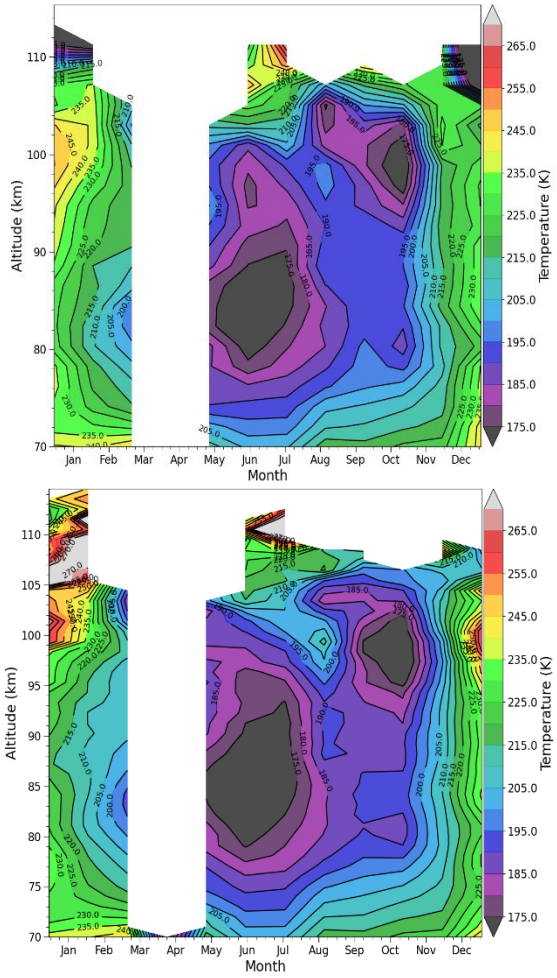

Figure 3.5: Temperature climatology using the upgraded RSL at USU which operated between 2014 and 2015. Top: OEM-reduced temperature climatology from data averaged by month. Bottom: Same as top but with HC-reduced temperatures.

(Sox, 2016; Argall, 2007), which also affects the Rayleigh-scatter cross section. Accordingly, this is not a likely cause for the differences we see. The OEM climtology shows cold temperatures high in the wintertime that may be related to the winter mesopause. This appears to be centered below 110 km, though due to insufficient nights of data we cannot define the mesopause for certain. Indeed in the HC plot there is no winter mesopause apparent. More and better data is needed from the high altitude system to attempt a study of the winter mesopause.

The summer mesopause can be seen clearly in both the HC and OEM climatologies, with minimum temperature regions plotted in

dark grey. This cold region is centered between May and August and is centered in altitude around 86 km in both plots. There is another large cold region centered at ~100 km and around mid-October, which can be seen in both plots as well. This region is likely the location of the mesopause during the fall of 2014. With this we can see that the low temperature mesopause region appears to ascend from summer to winter. We can see a hint of a cool region the OEM climatology of the original temperatures shown in Figure 3.1 between mid-October and December between 95 km and 100 km as well. However, because this is the top altitude limit of the original data set we cannot say for certain that these features are related or if a prominent fall mesopause would be present in other climatologies. More observations using the high-altitude lidar system is needed to confirm the existence of this fall feature.

Further comparisons between the OEM temperature climatologies from the original data and the newer data, Figure 3.1 and Figure 3.5 (top) respectively, we see some similarities in the overall climatology. However, the high altitude lidar temperatures show cooler temperatures in the summer mesopause than those of the low altitude lidar and warmer temperatures in January and December above 90 km. There are three main factors that might contribute to these differences. First, there is a somewhat significant number of years between the observations taken from the old lidar system and the new lidar system. At a minimum there were 10 years and at a maximum 21 years. There have been studies that show climate change may have an impact on temperature and dynamics in the atmosphere, which would likely propogate upwards in a coupled atmosphere (Roble and Dickinson, 1989; Solomon et al., 2018; Thomas, 1996). Furthermore, the upgraded lidar operated over a single year of the solar cycle, whereas the original lidar operated over a full solar cycle. This means that the averages could reflect a different period of the solar cycle than the single year (Friis-Christensen and Lassen, 1990; Hathaway, 2015). This idea is explored further in Chapter 5. Second, because the newer lidar system is much more powerful (~57 times larger power aperture product) than the old. The regions of difference would have smaller uncertainties with the newer system than with the older system. However, the third point is that there are significantly more nights being averaged using the older lidar data, which lessens the impact a single profile has on the overall climatology and results in smaller uncertainties in each profile. Whatever the cause for the differences may be, the new lidar system will be able to address these issues better by covering a greater altitude range with the larger mirrors, two lasers, and more efficient detectors. It will be used at every opportunity to start building another dense data set like the original set.

5. Discussion/conclusions

The OEM temperature climatologies show good agreement with the HC temperature climatologies, but with notable differences. These differences occur mainly at higher altitudes suggesting there is a common issue behind these differences. Other RSL groups have addressed an issue with the HC method in its reliance on a seed temperature at the topmost altitude. Sica and Haefele (2015) and others (Argall and Sica, 2007; Jalali et al., 2018) have discussed the need to remove the top 10 km to 15 km from the analysis due to the uncertainties and unknown biases introduced into the temperature reduction by using the HC method. This would lower the original lidar temperatures to a max altitude of ~85 km, which is significant. As described in Chapter 2, the OEM provides an advantage over HC in that the top altitude is statistically determined using the averaging kernel matrix to determine the point at which the a priori temperature becomes significant. At this altitude, and beyond, all temperatures are determined to be due to the a priori value rather than the relation to the observed RSL data. Thus, the data under

this altitude threshold is expected to be reliable. As such, these differences in analyses may prove to be the largest factor in the differences we are seeing between the OEM and HC temperature climatologies.

The location of the summer mesopause can be seen in both the old and newer climatologies to occur between 80 and 90 km centered around ~83 km in the old data and ~86 km in the newer data. We can see a secondary minimum temperature occurring during the fall in the newer lidar temperatures around 100 km. It is not clear if this is a feature unique to 2014 or whether it is a third mesopause, a fall mesopause. However, it does appear to show the low temperature region of the summer mesopause ascend upwards towards the winter mesopause. The newer lidar data shows minima in the winter occurring at or above 110 km. Again, due to lack of data during the winter and with the newer data set in general it is unclear if these values are reliable or if they only reflect the winter mesopause of 2014-2015. Published estimates of the location of the winter mesopause put it around 105 km (She et al., 2000; She and von Zahn, 1998; von Zahn et al., 1996). If the winter mesopause was indeed around 110 km in 2014, it would indicate a much warmer winter mesosphere and may provide an interesting study into how tropospheric weather (affecting all life) is reflected in the mesospheric temperature behavior. With few instruments capable of observing this region of the mesosphere this may be challenging. However, a collaborative study with another lidar group such as the one at UWO might prove interesting. Another resource that may be useful is the possibility of comparisons with the SABER instrument aboard NASA's TIMED satellite, which has been operating since January 2002. With the additional upgrades coming shortly to the USU RSL shortly, we expect the range of operation to cover from below 40 km to above 120 km and hope to add to this study by providing another high-quality, dense data set.

References

Ehard, Benedikt, Peggy Achtert, Andreas Dörnbrack, Sonja Gisinger, Jörg Gumbel, Mikhail Khaplanov, Markus Rapp, and Johannes Wagner. "Combination of Lidar and Model Data for Studying Deep Gravity Wave Propagation." *Monthly Weather Review* 144, no. 1 (January 1, 2016): 77–98. https://doi.org/10.1175/MWR-D-14-00405.1.

Ehard, Benedikt, Sylvie Malardel, Andreas Dörnbrack, Bernd Kaifler, Natalie Kaifler, and Nils Wedi. "Comparing ECMWF High-resolution Analyses with Lidar Temperature Measurements in the Middle Atmosphere." *Quarterly Journal of the Royal Meteorological Society* 144, no. 712 (April 2018): 633–40. https://doi.org/10.1002/qj.3206.

Emmert, J. T., D. P. Drob, J. M. Picone, D. E. Siskind, M. Jones, M. G. Mlynczak, P. F. Bernath, et al. "NRLMSIS 2.0: A Whole-atmosphere Empirical Model of Temperature and Neutral Species Densities." *Earth and Space Science*, September 17, 2020. https://doi.org/10.1029/2020EA001321.

FRIIS-CHRISTENSEN, E, and K LASSEN. "Length of the Solar Cycle: An Indicator of Solar Activity Closely Associated with Climate." *Geol. Soc. Am. Bull* 102 (1990): 174.

Hathaway, David H. "The Solar Cycle." *Living Reviews in Solar Physics* 12, no. 1 (December 2015): 4. https://doi.org/10.1007/lrsp-2015-4.

Hauchecorne, A., M. L. Chanin, and R. Wilson. "Mesospheric Temperature Inversion and Gravity Wave Breaking." *Geophysical Research Letters* 14, no. 9 (September 1987): 933–36. https://doi.org/10.1029/GL014i009p00933.

Hauchecorne, Alain, and Marie-Lise Chanin. "Density and Temperature Profiles Obtained by Lidar between 35 and 70 Km." *Geophysical Research Letters* 7, no. 8 (August 1980): 565–68. https://doi.org/10.1029/GL007i008p00565.

Hauchecorne, Alain, Marie-Lise Chanin, and P. Keckhut. "Climatology and Trends of the Middle Atmospheric Temperature (33–87 Km) as Seen by Rayleigh Lidar over the South of France." *Journal of Geophysical Research* 96, no. D8 (1991): 15297. https://doi.org/10.1029/91JD01213.

Herron, Joshua P. "MESOSPHERIC TEMPERATURE CLIMATOLOGY ABOVE UTAH STATE UNIVERSITY." All Graduate Theses and Dissertations, 2004. 6877. https://digitalcommons.usu.edu/etd/6877.

———. "Rayleigh-Scatter Lidar Observations at USU's Atmospheric Lidar Observatory (Logan,UT) - Temperature Climatology, Temperature Comparisons with MSIS, and Noctilucent Clouds." All Graduate Theses and Dissertations, 2007. 4686. https://digitalcommons.usu.edu/etd/4686.

Herron, Joshua, and Vincent B Wickwar. "Mid-Latitude Climatologies of Mesospheric Temperature and Geophysical Temperature Variability Determined with the Rayleigh-Scatter Lidar at ALO-USU." *Journal of Geophysical Research*, n.d., 59.

Jalali, Ali. "Validating and Highlighting the Advantages of the Optimal Estimation Method For Rayleigh Lidar Middle Atmospheric Temperature Retrievals." Electronic Thesis and Dissertation Repository, 2018. 5957. https://ir.lib.uwo.ca/etd/5957.

Jalali, Ali, Robert J. Sica, and Alexander Haefele. "Improvements to a Long-Term Rayleigh-Scatter Lidar Temperature Climatology by Using an Optimal Estimation Method." *Atmospheric Measurement Techniques* 11, no. 11 (November 8, 2018): 6043–58. https://doi.org/10.5194/amt-11-6043-2018.

Kafle, Durga N. "Rayleigh-Lidar Observations of Mesospheric Gravity Wave Activity above Logan, Utah." All Graduate Theses and Dissertations, 2009. 466. https://digitalcommons.usu.edu/etd/466.

Mwangi, MM, RJ Sica, and PS Argall. "Retrieval of Molecular Nitrogen and Molecular Oxygen Densities in the Upper Mesosphere and Lower Thermosphere Using Ground-based Lidar Measurements." *Journal of Geophysical Research: Atmospheres* 106, no. D10 (2001): 10313–23.

Roble, R. G., and R. E. Dickinson. "How Will Changes in Carbon Dioxide and Methane Modify the Mean Structure of the Mesosphere and Thermosphere?" *Geophysical Research Letters* 16, no. 12 (December 1989): 1441–44. https://doi.org/10.1029/GL016i012p01441.

Rodgers, Clive D. *Inverse Methods for Atmospheric Sounding: Theory and Practice*. Vol. 2. World scientific, 2000.

She, C. Y., Songsheng Chen, Zhilin Hu, James Sherman, J. D. Vance, Vince Vasoli, M. A. White, Jirong Yu, and David A. Krueger. "Eight-Year Climatology of Nocturnal Temperature and Sodium Density in the Mesopause Region (80 to 105 Km) over Fort Collins, Co (41°N, 105°W)." *Geophysical Research Letters* 27, no. 20 (October 15, 2000): 3289–92. https://doi.org/10.1029/2000GL003825.

She, C. Y., and U. von Zahn. "Concept of a Two-Level Mesopause: Support through New Lidar Observations." *Journal of Geophysical Research: Atmospheres* 103,

no. D5 (March 20, 1998): 5855–63. https://doi.org/10.1029/97JD03450.

Sica, R. J., and P. S. Argall. "Seasonal and Nightly Variations of Gravity-Wave Energy Density in the Middle Atmosphere Measured by the Purple Crow Lidar." *Annales Geophysicae* 25, no. 10 (November 6, 2007): 2139–45. https://doi.org/10.5194/angeo-25-2139-2007.

Sica, R. J., and A. Haefele. "Retrieval of Temperature from a Multiple-Channel Rayleigh-Scatter Lidar Using an Optimal Estimation Method." *Applied Optics* 54, no. 8 (March 10, 2015): 1872. https://doi.org/10.1364/AO.54.001872.

Solomon, Stanley C., Han-Li Liu, Daniel R. Marsh, Joseph M. McInerney, Liying Qian, and Francis M. Vitt. "Whole Atmosphere Simulation of Anthropogenic Climate Change." *Geophysical Research Letters* 45, no. 3 (February 16, 2018): 1567–76. https://doi.org/10.1002/2017GL076950.

Sox, Leda. "Rayleigh-Scatter Lidar Measurements of the Mesosphere and Thermosphere and Their Connections to Sudden Stratospheric Warmings." All Graduate Theses and Dissertations, 2016. 5227. https://digitalcommons.usu.edu/etd/5227.

Thomas, G.E. "Global Change in the Mesosphere-Lower Thermosphere Region: Has It Already Arrived?" *Journal of Atmospheric and Terrestrial Physics* 58, no. 14 (October 1996): 1629–56. https://doi.org/10.1016/0021-9169(96)00008-6.

Wickwar, Vincent B., Thomas D. Wilkerson, Marc Hammond, and Joshua P. Herron. "Mesospheric Temperature Observations at the USU/CASS Atmospheric Lidar Observatory (ALO)." edited by Upendra N. Singh, Toshikasu Itabe, and Nobuo Sugimoto, 272. Sendai, Japan, 2001. https://doi.org/10.1117/12.417056.

Wing, Robin, Alain Hauchecorne, Philippe Keckhut, Sophie Godin-Beekmann, Sergey Khaykin, and Emily M. McCullough. "Lidar Temperature Series in the Middle Atmosphere as a Reference Data Set – Part 2: Assessment of Temperature Observations from MLS/Aura and SABER/TIMED Satellites." *Atmospheric Measurement Techniques* 11, no. 12 (December 18, 2018): 6703–17. https://doi.org/10.5194/amt-11-6703-2018.

Wing, Robin, Alain Hauchecorne, Philippe Keckhut, Sophie Godin-Beekmann, Sergey Khaykin, Emily M. McCullough, Jean-François Mariscal, and Éric d'Almeida. "Lidar Temperature Series in the Middle Atmosphere as a Reference Data Set – Part 1: Improved Retrievals and a 20-Year Cross-Validation of Two Co-Located French Lidars." *Atmospheric Measurement Techniques* 11, no. 10 (October 10, 2018): 5531–47. https://doi.org/10.5194/amt-11-5531-2018.

Zahn, U. von, J. Höffner, V. Eska, and M. Alpers. "The Mesopause Altitude: Only Two Distinctive Levels Worldwide?" *Geophysical Research Letters* 23, no. 22 (November 1, 1996): 3231–34. https://doi.org/10.1029/96GL03041.